

# Variability in aerosol optical properties at Hornsund, Spitsbergen\*

OCEANOLOGIA, 52 (4), 2010.  
pp. 599–620.

© 2010, by Institute of  
Oceanology PAS.

## KEYWORDS

Arctic aerosols  
Aerosol optical thickness  
Backward trajectory  
Meteorological conditions  
Hornsund, Spitsbergen

ANNA ROZWADOWSKA<sup>1,\*</sup>  
PIOTR SOBOLEWSKI<sup>2</sup>

<sup>1</sup> Institute of Oceanology,  
Polish Academy of Sciences,  
Powstańców Warszawy 55, PL-81-712 Sopot, Poland;  
e-mail: ania@iopan.gda.pl

\*corresponding author

<sup>2</sup> Institute of Geophysics,  
Polish Academy of Sciences,  
Księcia Janusza 64, PL-01-452 Warsaw, Poland

Received 20 September 2010, revised 21 October 2010, accepted 15 November 2010.

## Abstract

Spectra of the aerosol optical thickness from the AERONET station at Hornsund in 2005–2008 were employed to study the interseasonal and intraseasonal variability in aerosol optical thickness for  $\lambda = 500$  nm (AOT(500)) and the Ångström exponent in the southern part of Spitsbergen in spring and summer. The dependences of aerosol optical properties on long-range transport and local meteorological conditions, i.e. wind direction and speed and humidity, were analysed. Backward trajectories computed by means of the NOAA HYSPLIT model (Draxler & Rolph 2003) were used to trace the air mass history. The mean values of AOT(500) for spring and summer were  $0.110 \pm 0.007$  (mean and standard deviation of the mean) and  $0.048 \pm 0.003$  respectively. The average values of the Ångström exponent do not differ and

---

\* This research was carried out as part of the statutory programme of the Institute of Oceanology PAN in Sopot, Poland (No. I.1.1/2010).

take respective values of  $1.44 \pm 0.03$  and  $1.45 \pm 0.03$ . In both seasons, the highest AOT(500) cases (the highest 20% of AOT values) can be explained by long-range transport from Europe, Asia (spring and summer) and North America (summer). In summer, the impact of distant sources on AOT is strongly modified by cleansing processes en route to Hornsund. Local meteorological conditions at the station are of secondary importance as regards the intraseasonal variability of aerosol optical properties in the southern part of Spitsbergen.

## 1. Introduction

Aerosol optical properties vary in both space and time. In the Arctic, seasonal variations are especially strong. Seasonality of AOT, i.e. higher values of AOT during spring – the Arctic haze season – and lower values during summer months, is observed at various Arctic stations (Tomasi et al. 2007). In the Arctic, AOT(500) varies from 0.12 to over 0.35 in the presence of Arctic haze to less than 0.1 and often less than 0.05 on clean days in summer (Tomasi et al. 2007, Stone et al. 2010).

The seasonal variability of aerosol optical properties results from variability in aerosol load, composition and size distribution (Herber et al. 2002, Tomasi et al. 2007). Aerosol regimes in spring and summer differ considerably from each other with respect to chemical composition and particle size distribution of aerosols. In late winter and spring, aged particles, i.e. accumulation-mode particles (diameters of 90–630 nm), dominate the number density distribution of the submicron fraction of aerosol at the Zeppelin station, Spitsbergen. In summer conditions, Aitken-mode particles (diameters of 22–90 nm) are the most numerous (Ström et al. 2003, Engvall et al. 2008). At Barrow, Alaska, sulphate aerosol dominates light scattering by submicron particles during the spring Arctic haze season. In summer, sulphate and sea salt both contribute to the submicron scattering. Scattering by supermicron particles tends to be dominated by sea salt and is most important in summer because of the break up of the sea ice (Quinn 2002, Tomasi et al. 2007).

Advection of anthropogenic pollutants, biomass burning aerosol, dust and volcanic aerosol from lower latitudes has a strong impact on the aerosol load in the Arctic (Nagel et al. 1998, Stohl et al. 2006, Generoso et al. 2007, Stone et al. 2007, Tomasi et al. 2007, Treffeisen et al. 2007, Law & Stohl 2007, Hirdman et al. 2010). Long-range transport of aerosols and their gaseous precursors is most abundant in winter and spring, when the southward shift of the polar front facilitates the advection of polluted air from mid-latitudes, mainly from Europe and Asia. The effectiveness of transport of aerosols and their gaseous precursors is additionally enhanced by a stable atmosphere and relatively low scavenging by clouds and precipitation (Quinn et al. 2007 and the papers cited there). A cold,

stable atmosphere inhibits turbulent transfer between atmospheric layers and the formation of cloud systems and precipitation, the major removal pathway for particulates from the atmosphere. The end of the polar night causes the generation of aerosols from gaseous precursors as a result of photochemically induced reactions. In summer, advection of air from mid-latitudes is more difficult because the polar front moves further north. Moreover, in summer cleansing processes en route to the Arctic, e.g. dry deposition and aerosol scavenging by rain and clouds, are more effective (Law & Stohl 2007, Rozwadowska et al. 2010).

Natural aerosols of Arctic origin consist of sea salt particles (Petelski & Piskozub 2006), mineral dust, the oxidation products of dimethyl sulphide emitted from the sea surface (Hillamo et al. 2001), and insoluble organic particles derived from the surface microlayer of the ocean by bubble bursting (Leck & Bigg 2005a, Leck & Bigg 2005b). Local production of mineral dust can occasionally be intensive, as during the dust-storm event on 18–21 May 2004 in Adventdalen, Spitsbergen (Dörnbrack et al. 2010). Local natural sources are the most effective in summer, when the sea ice retreats and the snow on land at least partially melts. In general, however, their impact on AOT is less than the influence of long-range advection.

Although the features described above are characteristic of the whole Arctic, both temporal and spatial differences are observable (Hirdman et al. 2010). What is more, the contributions from different sources to vertical aerosol concentration may vary with altitude (Heidam et al. 2004, Shindell et al. 2008), which results in additional variability in aerosol properties.

In the present paper we study the variability in the aerosol optical thickness (AOT(500)) and Ångström coefficient in the southern part of Spitsbergen. Differences between the spring and summer seasons as well as intraseasonal variability are considered. Dependences of aerosol optical properties on long-range transport and local meteorological conditions (i.e. wind direction and speed, and humidity) in each season are also addressed.

The outline of the paper is as follows: section 2 describes the data and methods applied in this study. Section 3 presents the results. In section 3.1 AOT regimes are presented for spring (with Arctic haze) and summer at the Hornsund station. In section 3.2, the authors discuss the dependence of mean daily AOT and Ångström exponent values on air mass advection. Section 3.3 analyses the possible influence of meteorological conditions at Hornsund on AOT(500). Section 4, the Conclusions, summarizes the findings.

## 2. Data and methods

Aerosol Optical Thickness (AOT) data from the AERONET (AErosol RObotic NETwork) station at Hornsund from the period 2005–2008 are employed in the present paper. The Hornsund station provided total Aerosol Optical Thickness (AOT) values for selected wavelengths (340, 380, 440, 500, 675, 870, 1020 nm) as well as contributions of the fine and coarse modes of aerosol size distribution to the total AOT for  $\lambda = 500$  nm ( $AOT_f(500)$  and  $AOT_c(500)$ ). The modes used in this instance by AERONET are defined optically (for details see O'Neill et al. 2003). For the purpose of this paper the authors used mainly AOT data.  $AOT_f(500)$  and  $AOT_c(500)$  were used in the quality assessment of AOT(500). The measurements in Hornsund were performed from late March to late September. Under clear skies the measurements were made 6 times an hour (intervals of 6–15 minutes between measurements). In cloudy conditions the measurements were unevenly distributed during the day.

The original spectra obtained from AERONET were additionally cloud-screened to remove the bias in AOT measurements due to the presence of thin Cirrus clouds and ice crystals blown off the ground (the fjord is surrounded by mountains). Since the authors did not have independent Cirrus cloud measurements for a further quality assessment, the nature of the temporal changes in AOT(500),  $AOT_f(500)$  and  $AOT_c(500)$  as well as meteorological observations were used. Cases when greater temporal variability in AOT was caused only by coarse particles and could not be justified by a storm on the ocean were rejected. They indicated the high probability of thin Cirrus clouds or drifting snow crystals. A more detailed description of AOT quality assessment can be found in Rozwadowska et al. (2010).

For each observation the Ångström exponent ( $\alpha$ ) was computed by a fitting method. The Ångström exponent is the slope of the AOT spectrum presented on the log-log scale. It is defined as

$$AOT(\lambda) = AOT(\lambda_0) \times \left( \frac{\lambda}{\lambda_0} \right)^\alpha, \quad (1)$$

where  $\lambda_0$  is the reference wavelength; in this paper  $\lambda_0 = 500$  nm.

Because of the occurrence of deviations of the real spectrum shape from the line on the log-log scale,  $\alpha$  was calculated for the spectral range 440–870 nm. Two main factors influence the error in the Ångström exponent of an individual spectrum: the above-mentioned spectrum shape deviation, and the error in the AOT( $\lambda$ ) measurement, which at low aerosol loads may reach several dozen percent. The AOT measurement accuracy – 0.02 for UV and 0.01 for VIS (Eck et al. 1999) – is comparable to the summer

background value of AOT(500) equal to 0.03. The error in  $\alpha$  calculations for an individual measurement varies from  $< 0.1$  for AOT(500)  $> 0.35$ , 0.3 for AOT(500) = 0.1, 0.4 for AOT(500) = 0.07 and increases strongly for lower values of AOT(500).

Days during which a minimum of five measurements were made were chosen for the subsequent analyses. For each day the mean Ångström exponent ( $\alpha$ ) and the mean AOT(500) were calculated. The uncertainties of daily mean AOT(500) are  $< 0.005$ , with the exception of a few cases of high AOT and significant daily variability. Typical uncertainties of the daily mean  $\alpha$  are 0.07 for AOT(500) = 0.12, 0.1 for AOT(500) = 0.07 and 0.2 for AOT(500) = 0.04. The average  $\alpha$  uncertainty is caused mainly by the daily variability and nonlinearity of the spectrum. Henceforth, AOT(500) and  $\alpha$  will respectively denote the daily means of AOT(500) and  $\alpha$  (440–870).

AOT(500) data for spring and summer have been divided into 5 groups limited by the 20th, 40th, 60th and 80th percentiles, i.e. quintiles ( $q_i$ ), of the respective AOT(500) distribution function. The groups are denoted as  $Q_i(\text{AOT})$ , where  $i = 1, \dots, 5$ . All the cases of AOT(500)  $\leq q_{20}$  belong to the first quintile, and all the cases of AOT(500)  $> q_{80}$  belong to  $Q_5$ .

Meteorological data from Hornsund, namely wind speed, wind direction and air humidity, were used in the present work. Hornsund is WMO station No. 01003; meteorological observations are made every 3 hours at standard times.

Backward trajectories used to trace the air history were computed by means of the NOAA HYSPLIT model (Draxler & Rolph 2003). The mid-point of the aerosol-measuring period on a given day was selected as the trajectory arrival time input to HYSPLIT on that day. The ‘Reanalysis’ database was used for the calculations. ‘Reanalysis’ in this case means the name of a data set in the HYSPLIT services to calculate trajectories, i.e. Global NOAA-NCEP/NCAR pressure level reanalysis data archives reprocessed into the HYSPLIT compatible format (NCAR/NCEP reanalysis project, Kalnay et al. 1996, Draxler et al. 2009). The global data are given on a latitude-longitude grid (2.5 degrees) at 17 pressure levels. The time resolution of the data is 6 hours.

The trajectories were calculated for three arrival heights: 1 km, 2.5 km and 5 km above sea level (but the air altitude during the passage to Hornsund could vary). These heights are comparable to those used by Engvall et al. (2008) for Ny Ålesund. The selection of 1 km as the lowest level resulted from the orography around the station. As the fjord is surrounded by mountains from 500 to 1000 m in height above sea level, lower trajectories will be significantly influenced by the orography. The 5 km level at the station is in the free troposphere (FT), and the 1 km height at the station is

likely to be in the boundary layer (BL). The boundary layer over Hornsund is not a typical Arctic BL over an ice-covered sea (Rozwadowska et al. 2010). The station is located at the mouth of the fjord to the warm ocean and is surrounded by a varied landscape: fjord and ocean, glaciers, tundra and rocks. The BL in Hornsund is probably similar to that in Kongsfjorden (Spitsbergen). Engvall et al. (2008), who defined the boundary layer limits using the height of the cloud tops, assumed the thickness of the boundary layer in Ny Ålesund (Kongsfjorden) to be ca 2 km for April to June.

A comparison of back-trajectories for Hornsund with the respective trajectories arriving simultaneously at points located about 60 km N, S, W and E of Hornsund demonstrated the good representativeness of Hornsund trajectories for a larger area (Rozwadowska et al. 2010).

### 3. Results and discussion

#### 3.1. Spring and summer AOT regimes

As in the whole Arctic, the spring and summer aerosol regimes in Hornsund differ considerably. The temporal variations in AOT during the measurement years in Hornsund are presented in Figure 1. The transition period from spring to summer conditions varies only slightly from year to year. For the years 2005–2008 the measurements from Julian days 80 to 147 (i.e. the last ten days of March, April and May) represent the spring regime,

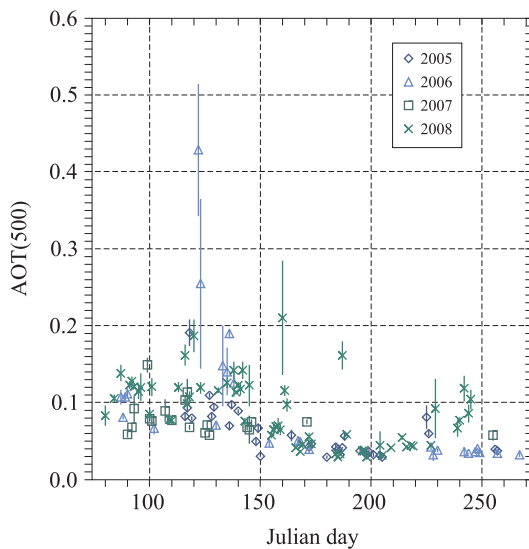


**Figure 1.** Temporal variability of AOT(500) from 2005 to 2008 in Hornsund. Symbols and whiskers show daily means and standard deviations (variability of AOT within a given day)

while the data for days 165–270 (i.e. mid-June to mid-September) represent summer conditions. This is in agreement with the findings for Ny Ålesund, Spitsbergen, by Engvall et al. (2008) that the transition from spring to summer conditions occurs in late May to early June each year and usually takes 10 days. From 2005 to 2008 several cases of extremely high AOT(500) were found. The highest AOT values noted on 2 and 3 May 2006 (respective Julian days 122 and 123; respective daily average AOT(500) 0.412 and 0.229) were caused by the extensive transport of pollution predominantly from farmland fires in Eastern Europe into the Arctic region (Myhre et al. 2007).

Seasonal differences in AOT(500) and the Ångström exponent in Hornsund are better illustrated by histograms (Figures 2a and b). The mean values of AOT(500) for spring and summer are equal to  $0.110 \pm 0.007$  (mean and standard deviation of the mean) and  $0.048 \pm 0.003$  respectively. Assuming that the average from the lowest 20% of AOT(500) during the season may be treated as the seasonal background, the difference between the summer and spring background AOT(500) is 100%. The respective background values are  $0.067 \pm 0.002$  and  $0.031 \pm 0.0004$ .

Seasonal means of AOT(500) in Hornsund are similar to the mean values of AOT(532) obtained by Herber et al. (2002) for tropospheric aerosols in Ny Ålesund, Spitsbergen, for 1991 to 1999:  $0.089 \pm 0.033$  (mean and standard deviation) for spring,  $0.046 \pm 0.024$  for summer, and  $0.031 \pm 0.014$  for autumn. To compute the tropospheric aerosol AOT, Herber et al. (2002) used the contribution of stratospheric aerosols to the total AOT(532) = 0.01

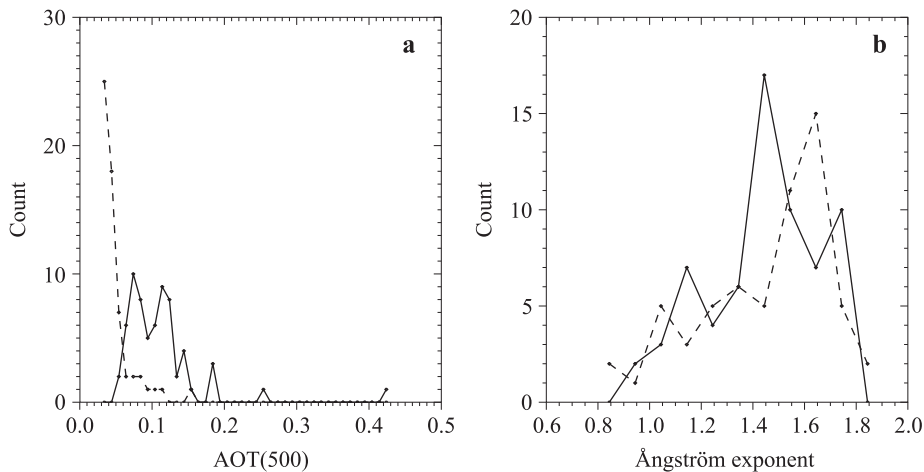
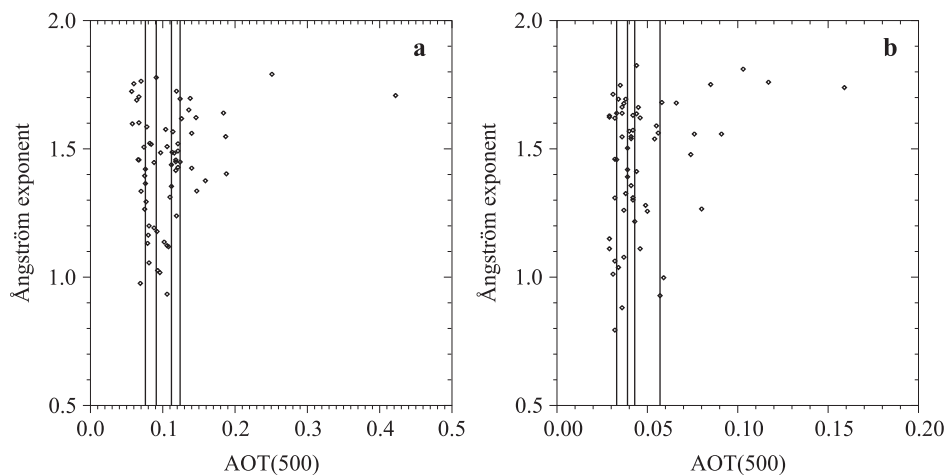


**Figure 2.** Histograms of AOT(500) (a) and Ångström exponent (b) for spring (solid line) and summer (dashed line). Measurements from Hornsund, 2005–2008

for the periods without volcanic activity. The spring mean of AOT(532) for tropospheric aerosols in cases without Arctic haze was  $0.067 \pm 0.017$  (mean and standard deviation), which is comparable to the spring background total (stratospheric+tropospheric) AOT(500) at Hornsund ( $0.067 \pm 0.002$ ; mean and standard deviation of the mean). According to Tomasi et al. (2007) the daily mean AOT(500) in Ny Ålesund in the presence of Arctic haze varied between 0.12 and 0.30 (1994–2006).

The seasonal average values of the Ångström exponent in Hornsund basically do not differ and take respective values of  $1.44 \pm 0.03$  and  $1.45 \pm 0.03$  for spring and summer (Figure 2b). The differences in modal values of the Ångström exponent were higher than in the case of the mean values. The modal values are 1.47 for spring and 1.62 for summer. As in Hornsund, the Ångström exponent in Ny Ålesund showed a seasonal pattern, its value being lower during spring and higher during the summer (2002–2005; Tomasi et al. 2007). In general, a high Ångström coefficient suggests the presence of small aerosol particles in the atmosphere. However, the value of the Ångström exponent must be interpreted with caution. It provides valid information about particle sizes only in cases of the Junge (1963) model of aerosol particle size distribution, whereas Arctic aerosols often have multimodal columnar size distributions, especially during episodes of Arctic haze, Asian dust, aged volcanic aerosols or boreal smoke (Tomasi et al. 2007). Because Arctic AOT spectra deviate from linearity on a log-log scale, any comparison of the Ångström exponent derived by different methods and/or for different wavelengths must be interpreted with caution (Tomasi et al. 2007). Unfortunately, there is a lack of long-term measurements of size distribution for the whole size range of aerosols in the Svalbard area. The only information available covers the aerosol diameter range from 20 to 630 nm (Zeppelin station, Ström et al. 2003). The shape of the distribution changes from an accumulation-mode dominant one in spring to a distribution dominated by the Aitken mode in summer. However, the contribution of the coarse mode to the seasonal variability of the total aerosol load and its impact on the Ångström exponent are unknown.

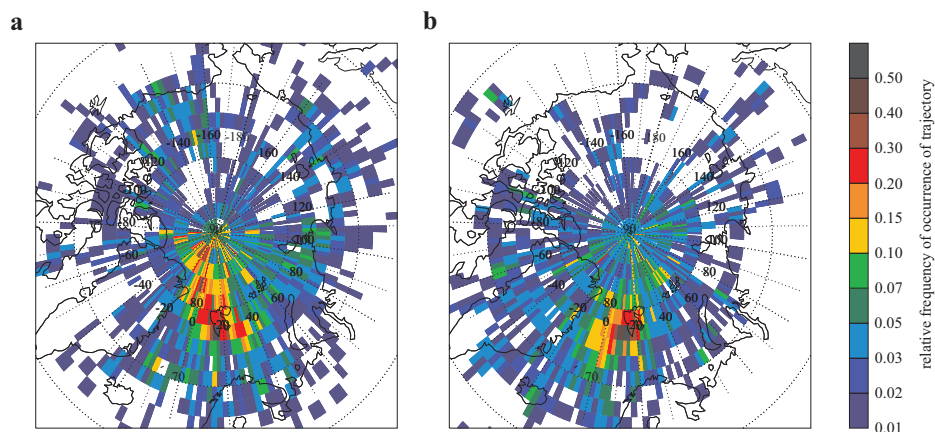
Figure 3 presents the dependence of the Ångström exponent on AOT(500) for the five quintile groups and for each season separately. In spite of seasonal differences in AOT values, the patterns of  $\alpha(\text{AOT}(500))$  for spring and summer are very similar: high variability in the Ångström exponent for lower groups and high  $\alpha$  values for  $Q_5$  ( $> 1.3$  for spring and  $> 1.2$  for summer). This suggests that high AOT cases are due to attenuation by small particles.



**Figure 3.** AOT(500) versus Ångström exponent for spring (a) and summer (b) in Hornsund. Vertical lines denote the 20th, 40th, 60th and 80th percentiles ( $q_i$ ) of the respective AOT distribution function

### 3.2. Impact of air back-trajectories on AOT

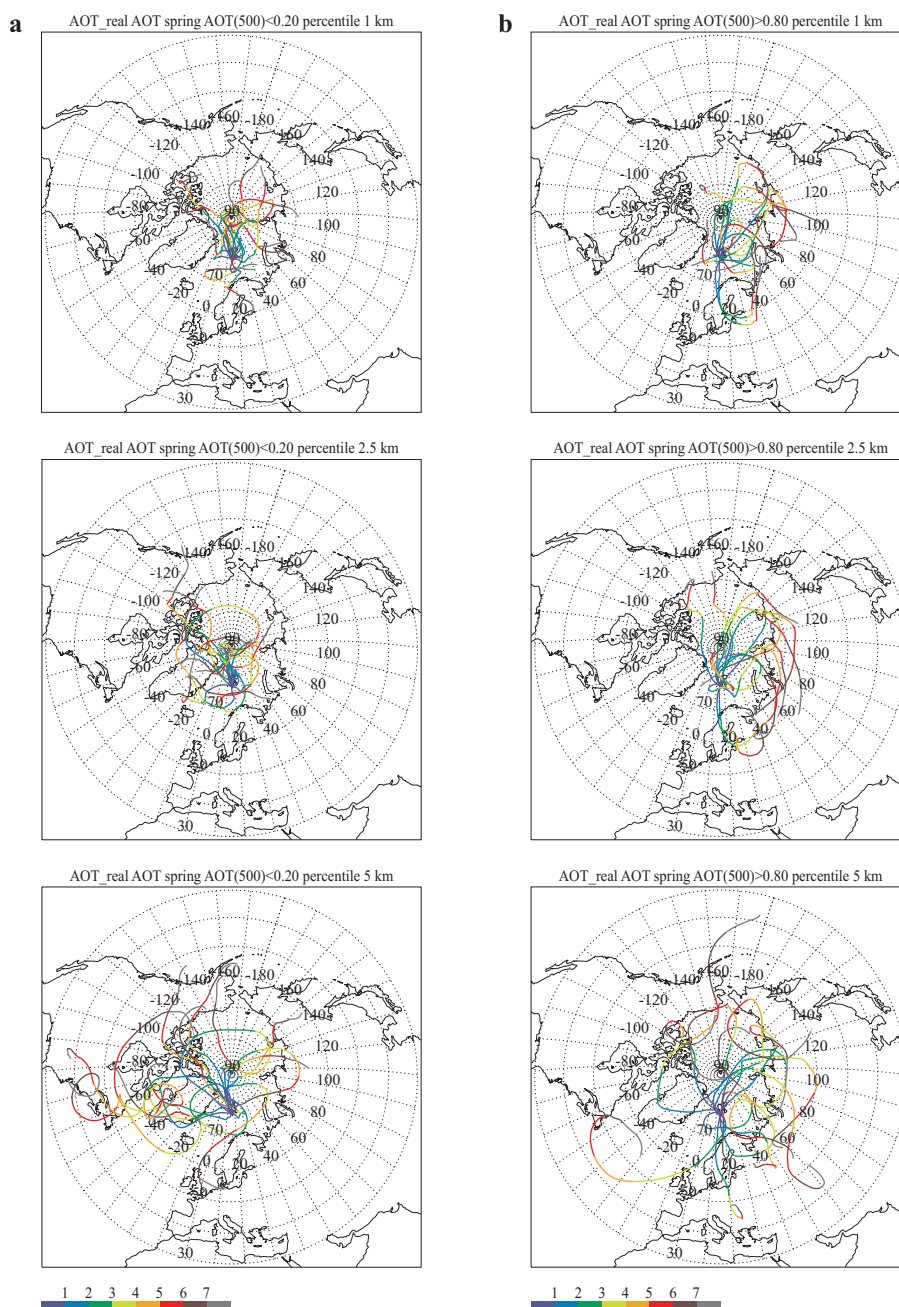
Rozwadowska et al. (2010) showed the importance of long-range transport for AOT(500) variability at Hornsund station. The atmospheric circulation is different in spring and summer (see section 1, Introduction).



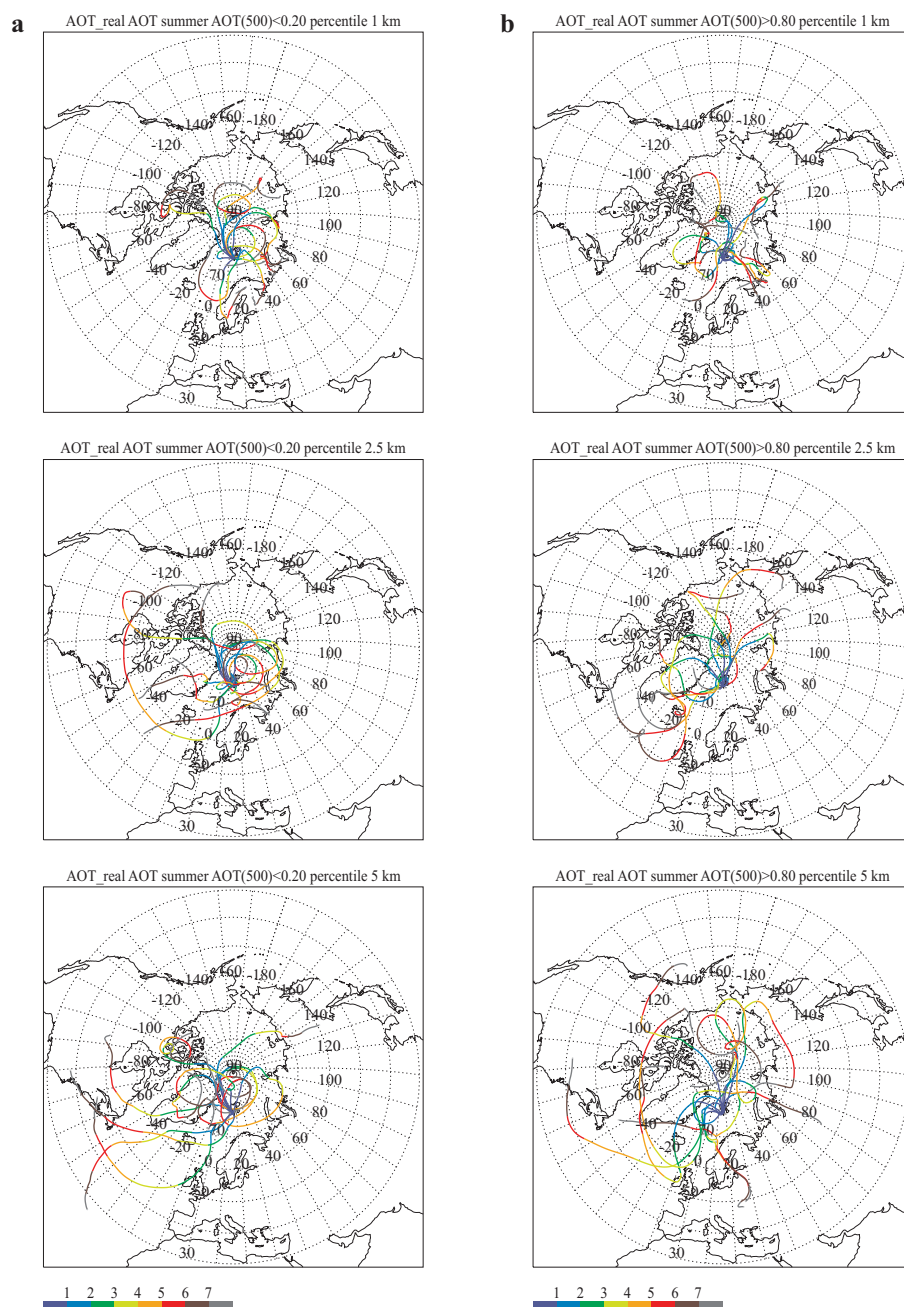
**Figure 4.** Spatial distributions of the frequency of occurrence of trajectories that reach Hornsund station at an altitude of 2500 m in spring (a) and summer (b) for days with AOT measurements. Frequency is expressed as the ratio of the total number of trajectory points (hours) belonging to a given sector in a given season to the number of trajectory points in the Hornsund sector in that season. The grey colour denotes frequency  $> 0.5$

Figure 4 shows spatial distributions of the frequency of occurrence of trajectories that reach Hornsund station at an altitude of 2500 m in spring (Figure 4a) and summer (Figure 4b) for days with AOT measurements. The frequency is expressed as the proportion of the total number of trajectory points (hours) that belong to a given sector in a given season to the number of trajectory points in the Hornsund sector in that season. Trajectory frequency values are corrected for latitudinal change in sector areas. Whereas in spring advection comes mainly from the northerly and easterly sectors, in summer the air inflow from the westerly sector (S-W-N) is dominant. This is consistent with findings by Eneroth et al. (2003), who analysed a 10-year data set of 5-day back-trajectories and pressure patterns for Ny Ålesund, Spitsbergen. It should be emphasized that our analysis applies only to days when AOT measurements were possible (i.e. days with sufficiently low cloud cover). In spring, i.e. mid-April to May, the typically persistent airflow from the Arctic and the slow transport from the northern part of Russia, Scandinavia and the Atlantic can be explained by the high pressure situation dominant over almost the whole Arctic region (Eneroth et al. 2003, Engvall et al. 2008). In summer (June, July and August), pressure gradients are weak, and long-range advectons are much less common than in spring; summer transport is also slower (Engvall et al. 2008, Law & Stohl 2007).

The atmospheric circulation influences the aerosol load and its optical properties. Rozwadowska et al. (2010) demonstrated considerable differences in mean aerosol optical properties among back-trajectory clusters for Hornsund. In the present paper, the authors studied the advection patterns for cases (days) belonging to particular quintile groups of AOT(500) distributions. Eight-day back-trajectories over Hornsund station were analysed for each quintile group and each season in Spitsbergen. Figures 5 and 6 show the trajectories of 20% of the lowest and the highest AOT(500) for spring (Figure 5) and summer (Figure 6). Table 1 presents the number of days of a given circulation type for cases that belong to AOT quintile groups 1–2 and 4–5. The classification of the synoptic situations is based on the calendar of circulation types for Spitsbergen compiled by Niedźwiedź (2009), which are determined on the day of trajectory arrival at Hornsund. The calendar uses surface synoptic maps and takes into account the direction of the geostrophic wind and the kind of pressure pattern (anticyclonic or cyclonic). The geostrophic wind direction illustrates the position of a cyclone or anticyclone with respect to southern Spitsbergen.



**Figure 5.** Back-trajectories of air that flows in over Hornsund at different heights for 20% of the lowest (a – left-hand panel) and the highest AOT (b – right-hand panel) cases in spring. The colours denote the number of days prior to reaching Hornsund



**Figure 6.** Back-trajectories of air that flows in over Hornsund at different heights for 20% of the lowest (a – left-hand panel) and the highest AOT (b – right-hand panel) cases in summer. The colours denote the number of days prior to reaching Hornsund

**Table 1.** Atmospheric circulation types and directions according to the circulation classification for Hornsund by Niedźwiedź (2009) for spring and summer as well as AOT quintile groups 1–2 (low AOT(500)) and 4–5 (high AOT(500)); a and c – anticyclonic and cyclonic situations respectively; N, NE, E, SE, S, SW, W and NW – directions of air mass advection (geostrophic wind); Ca – central anticyclone situation (high centre); Ka – anticyclonic wedge or ridge of high pressure; Cc – central cyclonic situation (centre of low); Bc – trough of low pressure (different directions of air flow and frontal system in the axis of the trough); x – unclassified situations

Season	AOT quintile group	Circulation type	Circulation direction												
			N	NE	E	SE	S	SW	W	NW	C	K	B	x	
Spring	1–2	c	5	3	2	2							x	2	
		a	4	2	4			1		1			x	2	
	4–5	c	3	1	1		1						x		
		a	3	8	3		2		1				3	x	
	Summer	1–2	c	2	2	1						3	1	x	1
			a			2		1	1	2	3			6	x
4–5		c	4		3			1		1			x	3	
		a	2	2	1		1			2	2	3		x	

### 3.2.1. Spring

In quintile group 1 ( $Q_1$ ), which has the lowest AOT ( $\langle \text{AOT}(500) \rangle = 0.067 \pm 0.002$ ), typical trajectories arriving at altitudes of 1 and 2.5 km run from the Greenland and Barents Sea areas, the Arctic Ocean (Nansen Basin and Amundsen Basin) and northern Canada (Figure 5a). The air remains in the Arctic for 7 or 8 days. At 5 km advection is mainly from northern Canada and Alaska, and the air typically stays in the Arctic for 3–7 days and arrives at the station from NW-NE sector. In  $Q_2$  ( $\langle \text{AOT}(500) \rangle = 0.082 \pm 0.001$ ) air masses come to Hornsund mainly from W-N-NE (not shown in Figure 5). In comparison to  $Q_1$ , the 1-km trajectory range extends farther, to the Chukchi Sea. Trajectories arriving at altitudes of 2.5 and 5 km above the station may be local, but they may also have come from the Pacific Ocean, Siberia, China, Canada and Alaska. In group 3 ( $\langle \text{AOT}(500) \rangle = 0.103 \pm 0.002$ ) at 1 and 2.5 km air arrives at the station from the NW-E. At 1 km the trajectories run from the Nansen Basin and Amundsen Basin, Barents Sea and the northern edges of Siberia. At 2.5 km the air

comes mainly from Siberia and at 5 km typically from Asia and Europe as far as 50–60°N. In quintile group 4 ( $\langle \text{AOT}(500) \rangle = 0.119 \pm 0.001$ ) air mass advection is mainly from W-N-E. A high variability in trajectories, i.e. different source regions of advection, is observed. In group 5, with maximum AOT values ( $\langle \text{AOT}(500) \rangle = 0.182 \pm 0.022$ ), back-trajectories come mainly from central and eastern Siberia and Europe (Figure 5b). Advection to the station is from the north or via a shorter route from the south.

Summing up, in the case of low AOT, lower level air masses typically stay over the Arctic Ocean and the adjacent seas, while the upper ones flow in from above North America. For the lowest AOT(500) cases ( $Q_1$ ) a few cases of advection from Europe and Asia have been found, usually at 5 km. With increasing AOT, the contribution of air masses from Europe and Asia grows at each altitude, being most pronounced at altitudes of 2.5 and 5 km. The highest AOT(500) cases can be explained by advectations from Asia and Europe.

Days with high AOT(500) ( $Q_4$  and  $Q_5$ ) and low AOT ( $Q_1$  and  $Q_2$ ) also differ considerably with respect to the Niedźwiedź (2009) circulation type on the day of air mass arrival at the Hornsund station (Table 1). Cyclonic and anticyclonic situations are equally frequent in quintile groups 1 and 2 during AOT measurements and flow (geostrophic wind) from sector N-E is dominant (20 out of 26 cases). In groups 4 and 5 a N-E circulation is also dominant (19/26), but an anticyclonic circulation prevails (20/26). The favouring of pollution advection by anticyclonic circulation is in agreement with previous findings for other parts of the Arctic.

### 3.2.2. Summer

Figure 6 presents the air mass trajectories of 20% of the lowest (Figure 6a) and highest AOT(500) cases (Figure 6b) for summer. The average AOT(500) values for quintile groups 1–5 are as follows:  $0.0307 \pm 0.0004$  (average of 20% of the lowest AOT(500)),  $0.0312 \pm 0.0005$ ,  $0.041 \pm 0.0004$ ,  $0.048 \pm 0.001$  and  $0.085 \pm 0.009$  (average of 20% of the highest AOT(500)).

In summer, the range of back-trajectories to Hornsund is lower than in spring. For the lowest AOT(500) (groups  $Q_1$  and  $Q_2$  with nearly identical mean AOT) air masses are mostly local, from the Arctic Ocean and Nordic seas (Greenland, Norwegian and Barents Seas). At altitudes of 2.5 and 5 km air advectations from over Canada and the North Atlantic were found. Some trajectories also lead from Europe and Asia. One-day-long trajectories typically come to Hornsund from the N-W-SW sector. The mean AOT group ( $Q_3$ ) is also related to air mass advectations from over the North Atlantic and Canada and direct inflow to the station from the N-W-SW

sector (one-day trajectories). Some trajectories run from Europe and Asia. Cases of the highest AOT(500) ( $Q_5$ ) are often related to advections from over Europe, Asia and North America. Such advections are less common than in spring. One-day trajectories in this group are mainly from the NW-NE.

According to the classification by Niedźwiedź (2009), anticyclonic situations are slightly more frequent (15/25) than cyclonic ones (10/25) in quintile groups 1 and 2. Circulations from the NW-E are dominant in cyclonic situations, whereas in anticyclonic situations air flows to Hornsund from the S-W-NW (from over the sea) and anticyclonic wedges or ridges of high pressure prevail. In cases of high AOT ( $Q_4$  and  $Q_5$ ), anticyclonic and cyclonic circulations are equally probable and the dominant flow direction for both anticyclonic and cyclonic situations is from the NW-E sector, that is, the air is likely to cross the island before reaching Hornsund.

High AOT(500) cases and low AOT(500) cases differ in both the air mass source area and the direction of the geostrophic wind (circulation pattern) on the day of arrival of the air mass at the station. This finding is in agreement with the previous study by Rozwadowska et al. (2010). They showed that although the main reason for elevated AOT in summer is long-range advection from the continents, AOT(500) variability depended strongly on the direction of air mass advection to the station, which can be explained by the spatial variability of the effectiveness of cleansing processes en route to Hornsund, i.e. dry deposition, wet deposition due to clouds and precipitation, and marine aerosol cleansing, i.e. aerosol scavenging by sea spray.

### 3.3. Impact of meteorological conditions on AOT

In this section we examine the dependence of AOT(500) on local meteorological conditions at Hornsund, i.e. air humidity, wind speed and wind direction. We want to determine the meteorological conditions for the highest and the lowest AOT(500) cases. The dependence of AOT(500) and  $\alpha(440-870)$  on the meteorological conditions at Hornsund is given in Figure 7. Wind speed and humidity are the values averaged over the AOT measurement period on a given day, and wind directions are taken from the meteorological observation station closest to the central point of AOT measurement period on a given day.

During the AOT measurements at the Hornsund station in spring, the relative humidity ranged from 49 to 87% and the wind speed did not exceed  $10 \text{ m s}^{-1}$ . In summer, the daily mean relative humidity calculated for AOT measurement periods was slightly higher than in spring and varied from 55 to 95%. The highest mean wind speed was  $12 \text{ m s}^{-1}$ . In both seasons, the

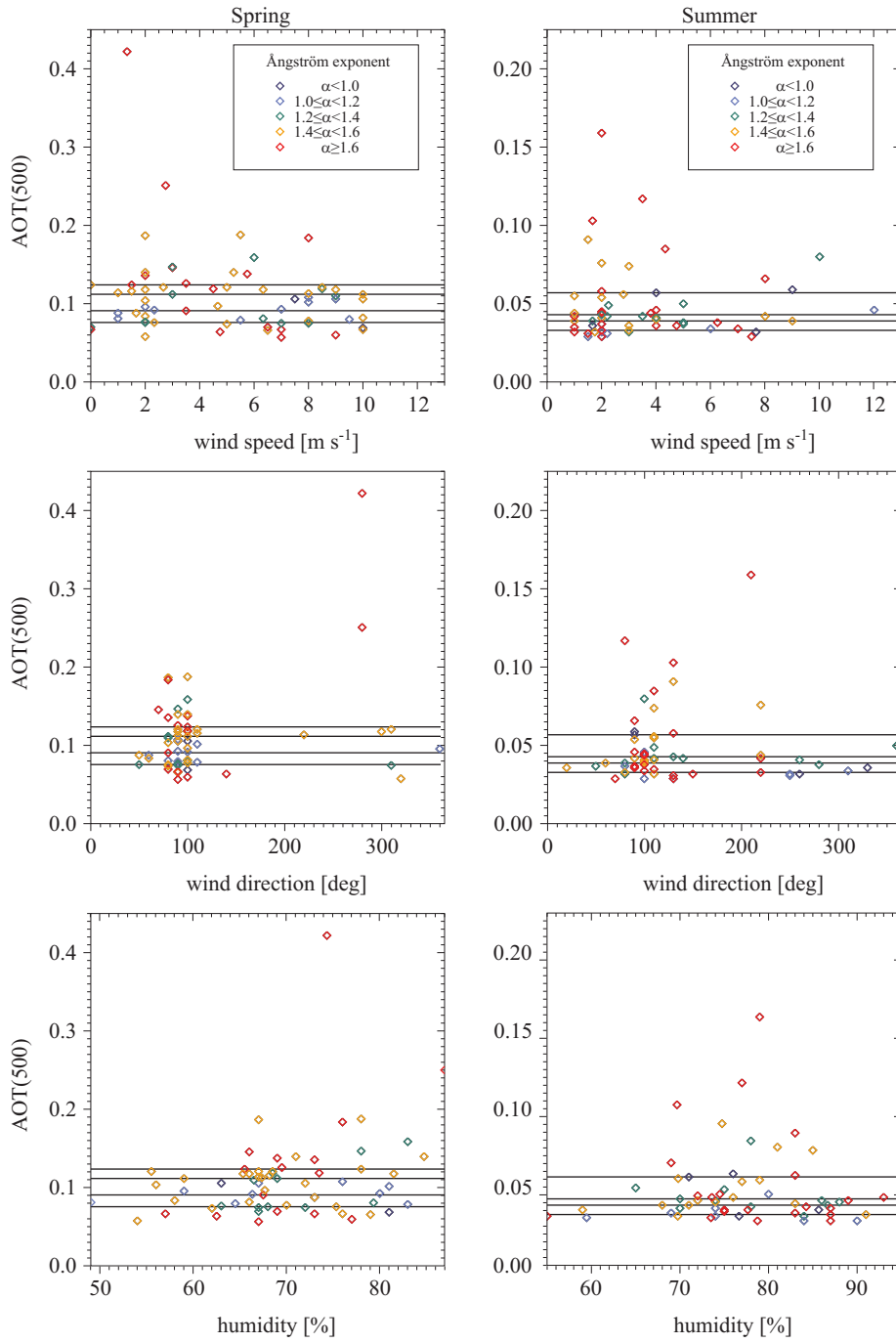


**Figure 7.** Dependence of AOT(500) and  $\alpha(440\text{--}870)$  on meteorological conditions at Hornsund. Horizontal lines denote the 20th, 40th, 60th and 80th percentiles ( $q_i$ ) of the respective AOT distribution function. Colours denote the Ångström exponent: navy blue  $\alpha < 1.0$ , blue  $1.0 \leq \alpha < 1.2$ , green  $1.2 \leq \alpha < 1.4$ , orange  $1.4 \leq \alpha < 1.6$ , red  $\alpha \geq 1.6$

wind direction was mainly easterly. It must be borne in mind that the wind direction at the Hornsund station is strongly modified by the latitudinal location of the Hornsund fjord and is therefore not fully representative of air transport in the boundary layer.

In practice, the whole range of wind speed values was observed for each AOT(500) quintile group, both in spring and summer. However, most of the highest AOT(500) values were found for winds  $\leq 6 \text{ m s}^{-1}$ , when generation of the local marine aerosol is weak. Moreover, high AOT(500) values are associated with high  $\alpha(440\text{--}870)$ , typical of non-sea-spray aerosols.

In spring, no relation between wind direction and AOT(500) was found. For on-shore wind directions  $\alpha(440\text{--}870)$  values were high, most probably because of the typically low wind speed on such days and/or at least the partly frozen sea. In summer, the highest AOT(500) occurred for wind directions from 60–220 degrees (E and S winds). High values of AOT(500) occurred mainly with winds from the S and SE sector. In general, this is in agreement with the trajectory directions shortly before reaching Hornsund. Low AOT values were found for each wind direction. In summer, the wind direction had an impact on the Ångström exponent, which is typically low for W-N winds. For winds from the W sector, the air comes to the fjord from over the open sea.

While low AOT(500) values occur over the whole humidity range observed during measurements, air humidity is typically  $65\% < \text{RH} < 85\%$  for AOT(500)  $> q_{80}$ . Neither very high nor very low relative humidities are observed for  $Q_5$ . According to Zieger et al. (2010) an increase in RH from 60% to 80% can result in a doubling of the aerosol scattering coefficient of the summer Arctic aerosol, which indicates that elevated RH values can contribute to an increase in AOT. Low AOT for  $\text{RH} > 85\%$  can be explained by the more efficient cleansing (wet deposition) in such conditions. In 60% of cases when  $\text{RH} > 86\%$ , fog or precipitation were recorded in past weather or at some distance from the station during AOT observations. When  $\text{RH} < 86\%$  this proportion drops to 12%. An occurrence of low AOT in the whole range of RH excludes RH as the main reason for high AOT. This is also confirmed by the relatively high values of the Ångström exponent in the  $Q_5$  AOT group.

Low wind speed, winds from the N-E-S sector and the lack of a clear relation between AOT and RH confirm that in both seasons elevated AOT(500) cases are due mainly to advection at Hornsund. The impact of local meteorological conditions on AOT variability, though noticeable in some cases, is of secondary importance in comparison with advection. For example, in the case of onshore winds in summer, the mean Ångström exponent decreases slightly with increasing wind speed (not shown in the

paper). Nevertheless, it should be noted that these conclusions concern only cases of low cloud coverage, when AOT measurements were possible; moreover, they are based only on surface meteorological observations.

#### 4. Conclusions

Our findings can be summarized as follows:

As in the whole Arctic, the spring and summer aerosol regimes in Hornsund differ considerably. The respective mean AOT(500) values for spring and summer are  $0.110 \pm 0.007$  (mean and standard deviation of the mean) and  $0.048 \pm 0.003$ . The average values of the Ångström exponent are similar for both seasons but the differences in modal values are greater:  $\langle \alpha(440-870) \rangle_{\text{spring}} = 1.47$  and  $\langle \alpha(440-870) \rangle_{\text{summer}} = 1.62$ . Assuming that the average from the lowest 20% of AOT(500) during the season may be treated as the seasonal background, the respective background AOT(500) values are as follows:  $0.067 \pm 0.002$  and  $0.031 \pm 0.0004$ . These findings are consistent with the aerosol data presented by Herber et al. (2002) and Tomasi et al. (2007) for the northern Spitsbergen station of Ny Ålesund.

In spring, distinct differences in trajectories and the circulation pattern between low AOT(500) cases and high AOT(500) cases are observed. The mean AOT(500) varies from  $0.067 \pm 0.002$  for quintile group  $Q_1$  to  $0.182 \pm 0.022$  for  $Q_5$ . In the case of low AOT, lower level air masses remain in the Arctic for 7–8 days prior to reaching Hornsund and the upper ones (arriving at an altitude of 5 km above the station) are typically advected from above North America. With increasing AOT, the contribution of air masses from Europe and Asia grows at each altitude, being the most pronounced at altitudes of 2.5 and 5 km. The highest AOT(500) cases can be explained by advections from Asia and Europe. Days with high and low AOT(500) also differ considerably with respect to the atmospheric circulation pattern (classification by Niedźwiedź 2009) on the day of air mass arrival at Hornsund. In the lowest 40% of AOT cases (quintile groups  $Q_1$  and  $Q_2$ ) cyclonic and anticyclonic situations are equally frequent during AOT measurements, and air flow (geostrophic wind) from the N to E sector is dominant. In the highest 40% of AOT cases advection from N-E also dominates, but anticyclonic circulations prevail.

In summer, intraseasonal variability of AOT is lower and varies from  $0.031 \pm 0.0004$  to  $0.085 \pm 0.009$  for  $Q_5$ . The range of back-trajectories to Hornsund is diminished when compared to spring. The high AOT(500) cases and low AOT(500) cases differ in both the air mass source area and the geostrophic wind direction on the day of air mass arrival at the station. Differentiation in the cleansing effectiveness of air masses en route to Hornsund is very important (Rozwadowska et al. 2010). In the lowest

40% of AOT(500) cases ( $Q_1$  and  $Q_2$ ) air masses are mostly local, from the Arctic Ocean and Nordic seas; however, at altitudes of 2.5 and 5 km air also advects from over Canada, North Atlantic, Europe and Asia. One-day long trajectories typically come to Hornsund from the N-W-SW sector. Cases of the highest AOT(500) ( $Q_5$ ) are usually related to advections from over Europe, Asia and North America. According to the classification by Niedźwiedź (2009), anticyclonic situations are slightly more frequent than cyclonic ones in the lowest 40% of AOT(500) cases ( $Q_1$  and  $Q_2$ ). In cyclonic situations circulations from the NW-E are dominant, whereas in anticyclonic situations air flows to Hornsund from the S-W-NW (from over the sea) and anticyclonic wedges or ridges of high pressure prevail. In cases of high AOT ( $Q_4$  and  $Q_5$ ), anticyclonic and cyclonic circulations are equally probable; the dominant direction of flow is from the NW-E sector for both types of circulation.

The influence of local meteorological conditions at the station on AOT(500) is of secondary importance when compared to the impact of air mass advection. The highest AOT(500) values were recorded for a humidity of 65–87% and low wind speeds (typically  $< 6 \text{ m s}^{-1}$ ). Moreover, no clear relation between AOT and RH was found. A noticeable dependence of AOT(500) and the Ångström exponent on wind direction was observed in summer. N-W winds are related to relatively low AOT values and Ångström exponents, which shows the influence of the sea. However, it must be noted that these conclusions apply only to cases of low cloud cover when AOT measurements were possible.

## Acknowledgements

The authors wish to express their gratitude the NOAA Air Resources Laboratory (ARL) for providing the HYSPLIT transport and dispersion model and the READY website (<http://www.arl.noaa.gov/ready.html>) used in this publication. The authors thank Brent Holben, the P.I. of the AERONET station at Hornsund. The authors would also like to thank the Department of Polar and Marine Research of the Institute of Geophysics, Polish Academy of Sciences, for providing the meteorological data used in this paper.

## References

- Dörnbrack A., Stachlewska I. S., Ritter C., Neuber R., 2010, *Aerosol distribution around Svalbard during intense easterly winds*, Atmos. Chem. Phys., 10(4), 1473–1490.

- Draxler R. R., Rolph G. D., 2003, *HYSPLIT (HYbrid Single-Particle Lagrangian Integrated Trajectory) Model access via NOAA ARL READY Website*, <http://www.arl.noaa.gov/ready/hysplit4.html>, NOAA Air Resour. Lab., Silver Spring, MD.
- Draxler R., Stunder B., Rolph G., Stein A., Taylor A., 2009, *HYSPLIT4 user's guide*, Ver. 4.9, [http://www.arl.noaa.gov/documents/reports/hysplit-user\\_guide.pdf](http://www.arl.noaa.gov/documents/reports/hysplit-user_guide.pdf)
- Eck T. F., Holben B. N., Reid J. S., Dubovik O., Smirnov A., O'Neill N. T., Slutsker I., Kinne S., 1999, *Wavelength dependence of the optical depth of biomass burning, urban, and desert dust aerosols*, *J. Geophys. Res.*, 104 (D24), 31 333–31 350.
- Eneroth K., Kjellström E., Holmen K., 2003, *A trajectory climatology for Svalbard; investigating how atmospheric flow patterns influence observed tracer concentrations*, *Phys. Chem. Earth*, 28 (28–32), 1191–1203.
- Engvall A.-C., Krejci R., Ström J., Treffeisen R., Scheele R., Hermansen O., Paatero J., 2008, *Changes in aerosol properties during spring-summer period in the Arctic troposphere*, *Atmos. Chem. Phys.*, 8 (3), 445–462.
- Generoso S., Bey I., Attié J.-L., Bréon F.-M., 2007, *A satellite- and model-based assessment of the 2003 Russian fires: Impact on the Arctic region*, *J. Geophys. Res.*, 112, D15302, doi:10.1029/2006JD008344.
- Heidam N. Z., Christensen J., Wahlin P., Skov H., 2004, *Arctic atmospheric contaminants in NE Greenland: levels, variations, origins, transport, transformations and trends 1990–2001*, *Sci. Total. Environ.*, 331 (1–3), 5–28.
- Herber A., Thomason L. W., Gernandt H., Leiterer U., Nagel D., Schulz K. H., Kaptur J., Albrecht T., Notholt J., 2002, *Continuous day and night aerosol optical depth observations in the Arctic between 1991 and 1999*, *J. Geophys. Res.*, 107 (D10), 4097, doi:10.1029/2001JD000536.
- Hillamo R., Kerminen V.-M., Aurela M., Mäkelä T., Maenhaut W., Leek C., 2001, *Modal structure of chemical mass size distribution in the high Arctic aerosol*, *J. Geophys. Res.*, 106 (D21), 27 555–27 571.
- Hirdman D., Sodemann H., Eckhardt S., Burkhardt J. F., Jefferson A., Mefford T., Quinn P. K., Sharma S., Ström J., Stohl A., 2010, *Source identification of short-lived air pollutants in the Arctic using statistical analysis of measurement data and particle dispersion model output*, *Atmos. Chem. Phys.*, 10 (2), 669–693.
- Junge C. E., 1963, *Air chemistry and radioactivity*, Acad. Press, New York, 111–208.
- Kalnay E., Kanamitsu M., Kistler R., Collins W., Deaven D., Gandin L., Iredell M., Saha S., White G., Woollen J., Zhu Y., Leetmaa A., Reynolds R., Chelliah M., Ebisuzaki W., Higgins W., Janowiak J., Mo K. C., Ropelewski C., Wang J., Jenne R., Joseph D., 1996, *The NCEP/NCAR 40-year reanalysis project*, *Bull. Amer. Meteor. Soc.*, 77 (3), 437–470.
- Law K. S., Stohl A., 2007, *Arctic air pollution: Origins and impacts*, *Science*, 315 (5818), 1537–1540.

- Leck C., Bigg E.K., 2005a, *Biogenic particles in the surface microlayer and overlaying atmosphere in the central Arctic Ocean during summer*, *Tellus B*, 57(4), 305–316.
- Leck C., Bigg E.K., 2005b, *Source and evolution of the marine aerosol – A new perspective*, *Geophys. Res. Lett.*, 32, L19803, doi:10.1029/2005GL023651.
- Myhre C.L., Toledano C., Myhre G., Stebel K., Yttri K.E., Aaltonen V., Johnsrud M., Frioud M., Cachorro V., de Frutos A., Lihavainen H., Campbell J.R., Chaikovsky A.P., Shiobara M., Welton E.J., Tørseth K., 2007, *Regional aerosol optical properties and radiative impact of the extreme smoke event in the European Arctic in spring*, *Atmos. Chem. Phys.*, 7(22), 5899–5915.
- Nagel D., Herber A., Thomason L.W., Leiterer U., 1998, *Vertical distribution of the spectral aerosol optical depth in the Arctic from 1993 to 1996*, *J. Geophys. Res.*, 103(D2), 1857–1870.
- Niedźwiedź T., 2009, *A calendar of atmospheric circulation types for Spitsbergen*, A computer file, Univ. Silesia, Dept. Climatol., Sosnowiec, Poland.
- O'Neill N.T., Eck T.F., Smirnov A., Holben B.N., Thulasiraman S., 2003, *Spectral discrimination of coarse and fine mode optical depth*, *J. Geophys. Res.*, 108(D17), 4559, doi:10.1029/2002JD002975.
- Petelski T., Piskozub J., 2006, *Vertical coarse aerosol fluxes in the atmospheric surface layer over the North Polar Waters of the Atlantic*, *J. Geophys. Res.*, 111, C06039, doi:10.1029/2005JC003295.
- Quinn P.K., Miller T.L., Bates T.S., Ogren J.A., Andrews E., Shaw G.E., 2002, *A 3 year record of simultaneously measured aerosol, chemical and optical properties at Barrow, Alaska*, *J. Geophys. Res.*, 107(D11), 4130, doi:10.1029/2001JD001248.
- Quinn P.K., Shaw G., Andrews E., Dutton E.G., Ruoho-Airola T., Gong S.L., 2007, *Arctic haze: current trends and knowledge gaps*, *Tellus B*, 59(1), 99–114.
- Rozwadowska A., Zieliński T., Petelski T., Sobolewski P., 2010, *Cluster analysis of the impact of air back-trajectories on aerosol optical properties at Hornsund, Spitsbergen*, *Atmos. Chem. Phys.*, 10(3), 877–893.
- Shindell D. T., Chin M., Dentener F., Doherty R. M., Faluvegi G., Fiore A. M., Hess P., Koch D. M., MacKenzie I. A., Sanderson M. G., Schultz M. G., Schulz M., Stevenson D. S., Teich H., Textor C., Wild O., Bergmann D. J., Bey I., Bian H., Cuvelier C., Duncan B. N., Folberth G., Horowitz L. W., Jonson J., Kaminski J. W., Marmer E., Park R., Pringle K. J., Schroeder S., Szopa S., Takemura T., Zeng G., Keating T. J., Zuber A., 2008, *A multi-model assessment of pollution transport to the Arctic*, *Atmos. Chem. Phys.*, 8(17), 5353–5372.
- Stohl A., Andrews E., Burkhart J.F., Forster C., Herber A., Hoch S.W., Kowal D., Lunder C., Mefford T., Ogren J.A., Sharma S., Spichtinger N., Stebel K., Stone R., Ström J., Tørseth K., Wehrli C., Yttri K.E., 2006, *Pan-Arctic enhancements of light absorbing aerosol concentrations due to North American boreal forest fires during summer 2004*, *J. Geophys. Res.*, 111, D22214, doi:10.1029/2006JD007216.

- Stone R. S., Anderson G. P., Andrews E., Dutton E. G., Shettle E. P., Berk A., 2007, *Incursions and radiative impact of Asian dust in northern Alaska*, Geophys. Res. Lett., 34, L14815, doi:10.1029/2007GL029878.
- Stone R. S., Herber A., Vitale V., Mazzola M., Lupi A., Schnell R. C., Dutton E. G., Liu P. S. K., Li S.-M., Dethloff K., Lampert A., Ritter C., Stock M., Neuber R., Maturilli M., 2010, *A three dimensional characterization of Arctic aerosols from airborne Sun photometer observations: PAM ARCMIP, April 2009*, J. Geophys. Res., 115, D13203, doi:10.1029/2009JD013605.
- Ström J., Umegard J., Torseth K., Tunved P., Hansson H. C., Holmen K., Wismann V., Herber A., König-Langlo G., 2003, *One year of particle size distribution and aerosol chemical composition measurements at the Zeppelin Station, Svalbard, March 2000–March 2001*, Phys. Chem. Earth, 28 (28–32), 1181–1190.
- Tomasi C., Vitale V., Lupi A., Di Carmine C., Campanelli M., Herber A., Treffeisen R., Stone R. S., Andrews E., Sharma S., Radionov V., von Hoyningen-Huene W., Stebel K., Hansen G. H., Myhre C. L., Wehrli C., Aaltonen V., Lihavainen H., Virkkula A., Hillamo R., Ström J., Toledano C., Cachorro V. E., Ortiz P., de Frutos A. M., Blindheim S., Frioud M., Gausa M., Zielinski T., Petelski T., Yamanouchi T., 2007, *Aerosols in polar regions: A historical overview based on optical depth and in situ observations*, J. Geophys. Res., 112, D16205, doi:10.1029/2007JD008432.
- Treffeisen R., Tunved P., Ström J., Herber A., Bareiss J., Helbig A., Stone R. S., Hoyningen-Huene W., Krejci R., Stohl A., Neuber R., 2007, *Arctic smoke – aerosol characteristics during a record air pollution event in the European Arctic and its radiative impact*, Atmos. Chem. Phys., 7 (11), 3035–3053.
- Zieger P., Fierz-Schmidhauser R., Gysel M., Ström J., Henne S., Yttri K. E., Baltensperger U., Weingartner E., 2010, *Effects of relative humidity on aerosol light scattering in the Arctic*, Atmos. Chem. Phys., 10 (8), 3875–3890.